Investigation of Gravitational Energy Harvesters for IoT Power Supply in Freight Train Monitoring

Investigation of Gravitational Energy Harvesters for IoT Power Supply in Freight Train Monitoring

Mirco Lo Monaco, Caterina Russo, Aurelio Somà
POLITECNICO DI TORINO
Corso Duca degli Abruzzi 24
Turin, Italy
Tel.: +39 011 090 102

E-Mail: mirco.lomonaco@polito.it, caterina.russo@polito.it, aurelio.soma@polito.it

***Index Terms*—Electromagnetic energy harvester, Renewable energy systems, Battery charger, Sensor, Condition monitoring.**

***Abstract*—Recent advances in technology make energy harvesting a promising power supply solution for IoT devices. An electromagnetic gravitational energy harvester prototype for railway monitoring applications is proposed. The main components of the autonomous IoT sensorized node are described. Laboratory dynamic tests and simulations show the harvester resonance frequency and maximum scavenged power for supplying the node. Experimental vertical vibration data collected onboard of a freight railcar are used for harvester frequency tuning and real performance evaluation. The node power management and rectification system is studied to choose the best smoothing capacitor. Experimental battery charge tests under the real onboard excitations are performed and the duty cycle of the autonomous IoT node is defined.**

I. Introduction

Energy harvesting is an increasingly growing technique for the conversion of the unused ambient energy into electric energy to be stored. Energy harvesters (EHs) are renewable energy systems capable of exploiting different energy sources, such as solar, thermal, wind, waves, and vibrations. These generators are suitable for supplying low-power Internet of Things devices in different application fields, from industrial to healthcare, from transportations to smart homes [1]. Wireless Sensor Networks (WSNs) for remote monitoring applications is one of the most promising technology amongst IoT devices. The major challenge for the realization of a WSN is finding a reliable, adequate, sustainable and cost-effective power source for each node [2], [3]. The use of batteries is a common solution due to their size, availability, cost, and the possibility of sensor deployment in hard-to-reach areas of the monitored system. However, even with the power draw optimization for improvement of battery and device lifespan, the necessity of battery replacement is relatively frequent. Large-scale battery disposal is not anymore acceptable due the environmental crysis we are experiencing. Energy harvesting devices could be a valid alternative to the use of batteries, easily producing electricity from free renewable ambient energy with negligeable costs. Wireless sensor nodes powered by energy harvesters become autonomous systems that have almost infinite lifespan, minimizing environmental damage and maintenance. Moreover, the use of energy harvesters can be a solution in systems that do not guarantee the supply of electricity [4].

The authors' research is focused on the realization of a sustaniable network of AIoT systems in freight vehicles, combining EHs and WSNs, for structural monitoring to overcome the absence of onboard electric power. The monitoring system allows to perform Condition Based Maintenance (CBM) to reduce risks of freight train derailments and consequent environmental and social damages [5]. According to the 2022 Transport Statistics Annual Report, from 2017 to 2021 a total of 2.260 hazardous materials freight trains accidents happened in the United States of America [6].

The proposed energy harvesting device is a gravitational vibrational electromagnetic energy harvester (GVEH), exploiting the kinetic energy of vibrations due to the wheel-railroad contact during the freight train ride. The converted electric power is effectively stored in a rechargeable battery that supplies the sensor and communication units for remote monitoring [7], [8]. The aim of this paper is to experimentally test the GVEH potentiality of charging a 3.6 V button battery under real measured vibrations of a freight wagon. Section

II describes the configuration and characteristics of the AIoT device. Section III shows the numerical modeling technique for dynamic simulations of the energy harvester conversion performances. Section IV reports the experimental results of battery charge laboratory tests under real excitations of the freight railcar. Then, a duty cycle is defined for the supply of a sensorized evaluation board. Section V presents the conclusion of the research and the future works.

II. System configuration

The proposed AIoT node is a system made of six fundamental components:

- Energy harvester
- Power Management System (PMS)
- Storage unit
- Sensor unit
- Micro-controller unit (MCU)
- Communication unit (CU)

The generator is a GVEH, a special configuration of a vibrational electromagnetic energy harvester (VEH). VEHs exploit kinetic energy coming from ambient vibrations of structures or vehicles and convert it into electric energy. The conversion methodology is based on Faraday's law of voltage induction due to the time variation of the magnetic flux generated by the relative motion between a permanent magnet and a coil [9], [10]. GVEHs use non-linear magnetic suspensions instead of traditional mechanical springs to enhance the overall system durability, reliability, and conversion efficiency thanks to frequency bandwidth broadening [11]. Section III describes the analytical and numerical models of the GVEH for further explanation of the dynamics and working principle.

The energy generated by the GVEH must be stored in batteries or supercapacitors, requiring a preliminary conversion of the generated alternate current into continuous current. Energy storage is usually necessary due to some reasons: firstly, to provide continuous supply also in case of irregular power generation; secondly, to reach the prescribed energy threshold needed to supply the user. Considering the freight monitoring application, the excitation input to the GVEH is strongly variable, with long periods where the train stops at the stations. The main goal is to have a reliable system that is able to remotely communicate even when the GVEH is not working, thanks to an effecient duty cycle definition. Consequently, the GVEH generated power must be managed correctly with a PMS to effectively store it in the battery. A first attempt of the PMS realization involves a KBU 1010 bridge rectifier to perform AC-DC conversion, with a capacitor for signal smoothing and pulsation reduction [12], [13]. The rectified and stable DC signal is fed into a battery charger board (Adafruit industries MCP73833 LiPo-Li/Ion Charger), having as output the load and a 3.6V 45 mAh button Li-Ion rechargeable battery (Storage Unit). STEVAL-BCN002V1B sensor board is attached to the load end, and plays the roles of sensor unit, MCU and CU. The ST board has ultra-low-power consumption, compatible with the harvester performances, is equipped with different sensors for various applications, and features Bluetooth Low Energy (BLE) communication. Section IV reports the board power consumption, battery charge tests and the definition of the system duty cycle. Figure 1 shows the schematics of the AIoT system and components.

III. Harvester model

The AIoT node generator is a cylindrical one-degree-of-freedom (1DOF) GVEH. The main components of the GVEH include a suspended moving ring magnet, a fixed ring magnet at the bottom end, coils wrapped around a tube and an internal guide. The set of moving and fixed magnets constitute an asymmetric non-linear magnetic spring, given the presence of only one fixed magnet at the bottom end. These energy harvesters are called "gravitational" since they exploit gravity action as the restoring force of the magnetic spring. The asymmetric configuration has a peculiar non-linear "softening" behavior resulting in the reduction of the system natural frequency with increasing excitation amplitude [14]. The moving and fixed magnets of the suspension are made of NdFeB42. The device has five coils with same dimensions, number of turns, resistance, material (enameled copper), and cross-section diameter. The coils are placed along the tube at different heights to find the axial location of the coil that optimizes the generated power.

A. Analytical model

The analytical model of the generator consists of a 1DOF non-linear mass-spring-damper system. The seismic mass m of the system is the moving magnet which is suspended thanks to the repulsive force with the fixed magnet at the bottom. The non-linear stiffness k is a characteristic of the magnetic spring. The system damping coefficient has two components: mechanical due to viscous action of the air and friction (c_{vis}), electromagnetic due to the induction of parasitic currents in the coils (c_{em}) [15]. External vibrations excite the system generating oscillatory motions of the moving

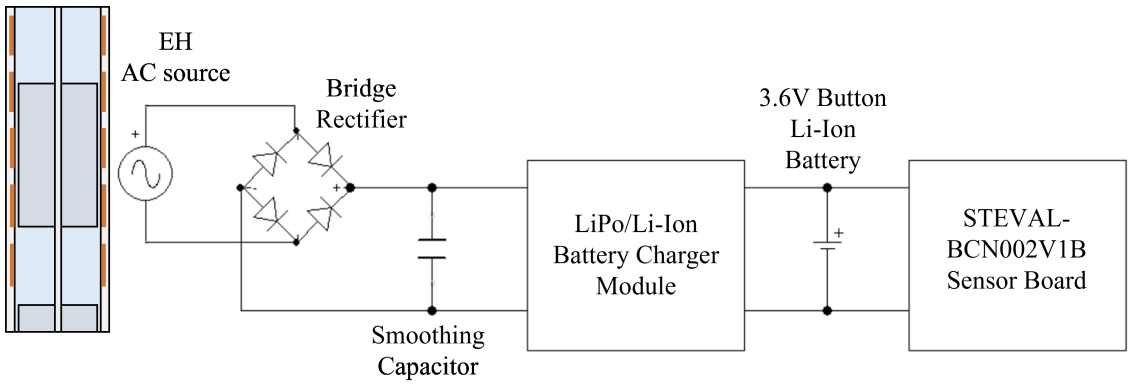

Fig. 1. AIoT system schematization.

magnet and starting the transducing mechanism. The time variation of the magnetic flux through the coils, due to the relative motion of the mass inside the tube, induces an electromotive force. The equation of motion of the system (1) is a second order differential equation expressed in the variable z, which is the relative motion coordinate of the moving magnet with origin in the equilibrium position.

$$\ddot{z} = -\frac{c_{tot}(z)}{m}\dot{z} - \frac{k(z)}{m}z + Y_0 \sin(\Omega t) \tag{1}$$

Where:

- z is the relative motion coordinate of the moving magnet;
- m is the seismic mass of the moving magnet;
- c_{tot} is the sum of viscous damping c_{vis} and electromagnetic damping c_{em};
- k is the non-linear stiffness of the magnetic spring;
- Y_0 is the external acceleration amplitude of sinusoidal input;
- Ω is the pulsation of the external excitation.

The transducing mechanism is based on an electromechanical coupling. The induced electromotive force is proportional to the moving magnet speed. Moreover, the induced current generates a non-linear damping force that influences the moving magnet motion. Subsequently, coil dimensions and resistance should be carefully designed to maximize the power generation and guarantee the correct dynamics. The electromagnetic subsystem is modeled as a purely resistive circuit where the harvester is the AC source, having an internal resistance R_{coil} , connected to the external resistance R_{load} that needs to be properly optimized for maximum power generation. The coil inductance can be neglected since R_{coil} is always significantly larger than the inductive impedance for frequencies under 1 kHz [16]. The scheme of the harvester analytical electro-mechanical model is reported in Figure 2.

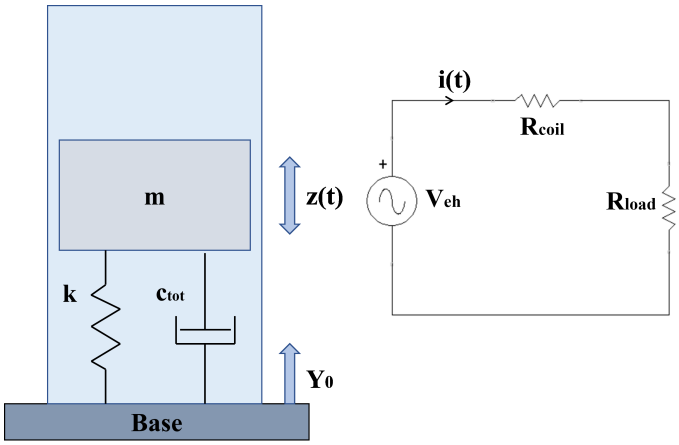

Fig. 2. Analytical electro-mechanical model of the harvester.

The electromagnetic coupling coefficient $k_{em}(z)$ derives from the variation of the magnetic flux during the moving magnet oscillation (2). The coefficient directly links the voltage to the moving magnet speed (3) and defines the non-linear electromagnetic damping characteristic acting on the moving mass (4).

$$k_{em}(z) = -\frac{d\Phi}{dz} \tag{2}$$

$$V_{eh} = -\frac{d\Phi}{dt} = -\frac{d\Phi}{dz}\frac{dz}{dt} = k_{em}\dot{z}(t) \tag{3}$$

$$c_{em}(z) = \frac{k_{em}^2(z)}{R_{coil} + R_{load}} \tag{4}$$

B. Numerical model

The characterization of the non-linear magnetic suspension and the time-variating magnetic flux requires

numerical simulations. The non-linearities arise from the dependance of both stiffness and damping characteristics on the relative moving magnet position. Ansys Maxwell FEM software is used for magnetostatic and transient electromagnetic simulations. For every position of the moving magnet, the software computes the corresponding repulsive force between the two magnets $F_{mag}(z)$ and the magnetic flux through the coils $\Phi(z)$. The derivation of both quantities respect to the relative moving magnet position z returns the magnetic spring stiffness $k(z)$ and the electromagnetic coupling coefficient $k_{em}(z)$, respectively. Figure 3 shows the curves of these two non-linear characteristics for the moving magnet stroke inside the tube. Electromagnetic coupling coefficient curves can be computed for each connected coil, resulting in the shifting of the maximum values along the moving magnet stroke. This behavior is crucial for evaluating the coil that maximizes the magnetic flux linkage during magnet oscillation.

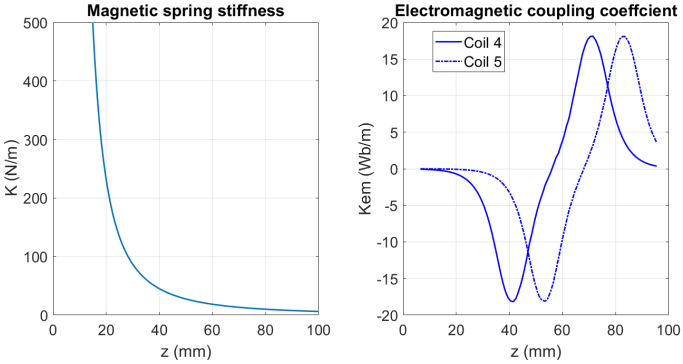

Fig. 3. Harvester non-linear numerical characteristics.

Equations (1)-(4) are implemented in a MATLAB/Simulink model for numerical dynamic simulations, thus evaluating the time response of the GVEH to the external sinusoidal excitation. The numerical characteristics of stiffness, electromagnetic coupling coefficient and damping are fed into the Simulink model. The output variables of the mechanical subsystem are the moving magnet position, speed, and acceleration. The mechanical variables are the input to the electromagnetic subsystem, resulting in the evaluation of the induced voltage, current, and generated power on the load.

IV. Experimental Results

Experimental tests must be carried out to evaluate the performance of the generator under different excitation inputs. A GVEH prototype has been designed for laboratory tests, with size and characteristics resulting from an optimization procedure [14]. Figure 4 shows a render image of the prototype, along with its dimensions. The GVEH is tested on a dynamic experimental workbench, featuring a shaker (TIRA TV51120), a DAQ with LabView software (National Instruments, Austin, TX, USA), an amplifier (BAA 500) with variable gain control (TIRA GmbH, Schalkau, Germany) and a piezoelectric accelerometer (PCB Piezotronics, Depew, NY, USA) for closed-loop feedback signal.

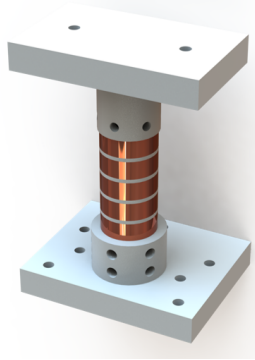

Tube height	100 mm
Tube diameter	26 mm
Moving magnet diameter	20 mm
Moving magnet height	30 mm
Fixed magnet diameter	20 mm
Fixed magnet height	5 mm
Coil number of turns	1500
Coil resistance	300 Ω

Fig. 4. GVEH prototype image and main dimensions.

A. Resonance frequency and maximum power

The first tests must concern the evaluation of the GVEH resonance frequency and corresponding power peak. GVEHs have maximum conversion efficiency at their natural frequencies, hence they should be designed to be tuned to the frequency range of the system vibrations fundamental excitation frequencies. Frequency Response Functions (FRFs) are computed performing frequency-sweep tests on the shaker, imposing sinusoidal excitations with different frequencies and amplitudes. The experimental FRFs are reported in Figure 5, obtained by imposing excitation inputs from 3 to 7 Hz with amplitudes from 0.2 to 0.5 g, and connecting the optimum coil to an external load of 430 Ω optimized resistance for maximum power generation. The non-linear softening behavior of the magnetic suspension results in the resonance frequency variation. Higher excitation amplitudes shift the resonance frequency to lower values. According to the FRFs curves, the high-power frequency bandwidth can be considered in the range from 3.5 Hz to 6 Hz. The maximum power generation, for an external excitation of 0.5 g, is of 32 mW at resonance frequency of 4.2 Hz.

B. Freight train vibrations analysis

The AIoT node is destined to freight trains remote monitoring applications. The GVEH generator scavenges

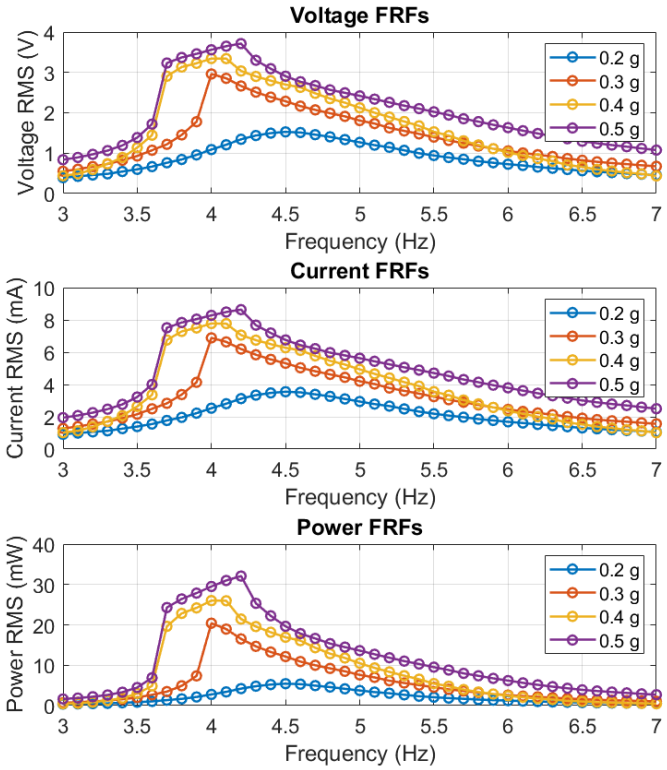

Fig. 5. Experimental FRFs.

the kinetic energy coming from freight wagons vibrations during the ride. Consequently, it is necessary to acquire real data of vertical accelerations on the freight wagon body during its working activity. These data are useful for the correct GVEH frequency tuning and to estimate the actual power that the generator can provide. The real acceleration data signal was collected with a data acquisition system of our research group, using a frequency sample of 200 Hz. The acceleration signal is processed to obtain the Fast Fourier Transform (FFT) and evaluate the fundamental frequencies of the train random excitation vibrations. As Figure 6 shows, the main frequencies of the wagon body, with load and at variable speeds, are 2 Hz and 4 Hz. This results confirms the correct tuning of the GVEH prototype, since its high-power frequency range is 3.5 to 6 Hz. The real acceleration data is fed into the Simulink block scheme to perform a dynamic simulation and estimate the GVEH power generation. The results are not satisfactory, since the excitation amplitudes on the wagon body are relatively low even at the main frequencies (about 0.04 g). The GVEH output RMS voltage is of 0.63 V, with a RMS current of 1.46 mA and 1.86 mW of RMS power. The installation site of the wagon body does not provide sufficient excitation amplitude due to the double suspension filters of the Y25 bogie. Consequently, a MultiBody model of the freight wagon is built to perform dynamic simulations and evaluate the excitation amplitudes at the bogie level. The freight wagon model is built in Simpack software (ideal for railway simulations) and simplified to estimate the order of magnitude of the acceleration amplification and consequently of the GVEH power. The model features the wheels and axle-box at the low end, the primary suspension that connects the axle-box to the bogie frame, the secondary suspension connecting the bogie frame to the wagon body, and the load on the body. The real acceleration signal is applied to the body to simulate the amplificated acceleration at lower level on the bogie. The bogie acceleration signal is then processed to obtain the FFT and evaluate the fundamental frequencies and corresponding amplitudes. As Figure 6 reports, the new fundamental frequencies on the bogie frame are around 8-9 Hz, with corresponding amplitude of about 0.4 g, ten times higher than the body. The frequency shift to higher value results in the detuning of the GVEH prototype. However, the excitation content in the GVEH range of 3.5-6 Hz is still higher at the bogie than the wagon body. Simulink simulations with the bogie acceleration input show a dramatic improvement of the GVEH performance, generating an RMS power of 21.5 mW, RMS voltage of 3.15 V, and RMS current of 7.33 mA.

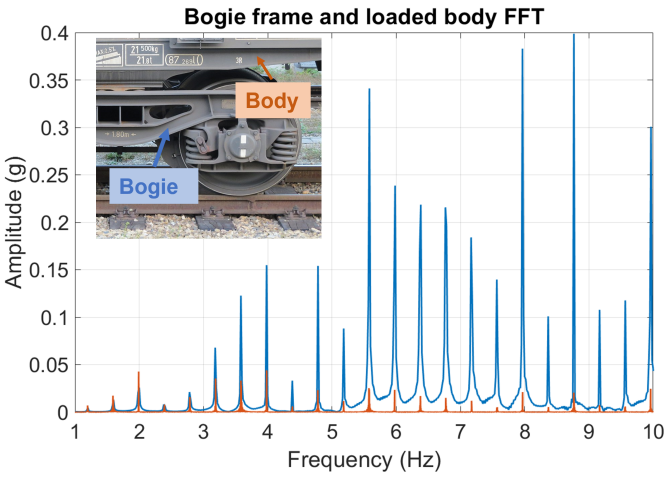

Fig. 6. Wagon bogie frame and body FFT.

C. Battery charge tests

The main purpose of the GVEH is to store power in a battery to guarantee constant supply to the sensor unit. Laboratory tests on the experimental setup described in Section IV must be performed to evaluate the GVEH battery charge process. Firstly, the PMS should be tested,

choosing the smoothing capacitor to correctly rectify the AC signal to DC and reduce its pulsation. The experimental tests are carried out imposing an ideal sinusoidal excitation having 0.5 g amplitude and the GVEH resonance frequency (Section IV-A). Three different aluminum electrolytic capacitors are tested and the respective output DC voltage signals are compared in terms of mean value and ripple. Figure 7 shows the experimental GVEH DC voltage signals with empty battery connected as a load. Details on the results are reported in Table I. The 2200 μF capacitor is chosen for the battery charge tests since is the best trade-off between high mean voltage and low ripple.

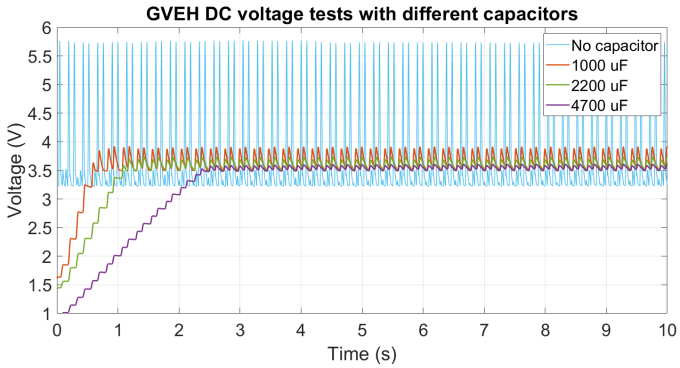

Fig. 7. GVEH DC voltage tests with different capacitors.

TABLE I
CAPACITOR TESTS RESULTS.

Capacity (μF)	Mean Voltage (V)	Ripple (V)
-	3.68	2.54
1000	3.67	0.41
2200	3.62	0.24
4700	3.57	0.11

Given the wagon body frame FFT obtained from Simpack simulations in Section IV-B, the main frequencies in the GVEH high-power range (3.5-6 Hz) and corresponding excitation content are applied to the GVEH on the experimental setup. Table II summarises the charging experimental tests settings and corresponding results. Figure 8 shows the charging curves of the 3.6 V Li-ion button battery resulting from the different experimental tests. The obtained curves have the typical pattern of the Li-Ion battery charge curves. Considering a time frame of one hour and a half, the battery reaches different levels of voltage, depending on the excitation input signal. In particular, with an input acceleration of 0.16 g - 4 Hz the battery voltage is 3.1 V, at 0.16 g - 4.7 Hz is 3.3 V and at 0.34 g - 5.8 Hz is 3.0 V. Figure 8 also shows the ideal charging curve with excitation input of 0.5 g and resonance frequency 4.2 Hz, reaching the battery voltage level of 3.7 V after 1.5 hours. During the experimental tests, the battery is charged with a variable voltage level depending on the excitation input applied to the GVEH. Following the GVEH FRFs in Section IV-A, a certain amount of power is provided by the generator and stored in the battery. Hence, the voltage level at which the battery is charged is depending on the excitation amplitude, which is variable during the working conditions of the GVEH on the train. Moreover, the electrical quantities of the GVEH depend on the load resistance of the battery, which changes during its charging phase. The GVEH output voltage increases with the external load resistance, growing as the battery charges, whereas the current decreases [17]. Consequently, the GVEH is capable of charging the battery up to a certain voltage level. The current decreases to a value not high enough to evaluate a significant charge of the battery in a time frame compatible with the charging speed needed for the application.

TABLE II
BATTERY CHARGE TESTS RESULTS.

Excitation	Duration (h)	Battery voltage (V)
0.16 g @ 4.0 Hz	1.5	3.1
0.16 g @ 4.7 Hz	1.5	3.3
0.34 g @ 5.8 Hz	1.5	3.0
0.50 g @ 4.2 Hz	1.5	3.7

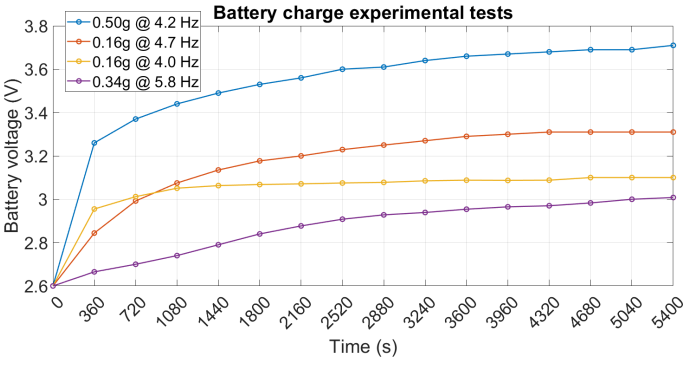

Fig. 8. Battery charge experimental tests.

D. Duty cycle definition

After the evaluation of the time required to partially charge the battery in different GVEH working conditions, it is now fundamental to understand the

power consumption of the sensor unit. The GVEH sizing cannot be separated from the detailed knowledge of the sensing/monitoring system that must be powered.

The chosen sensor unit is the STEVAL-BCN002V1B provided by ST that features different sensors, BLE connection, and has ultra-low power consumption. Figure 9 shows the sensor average power consumption for different activities.

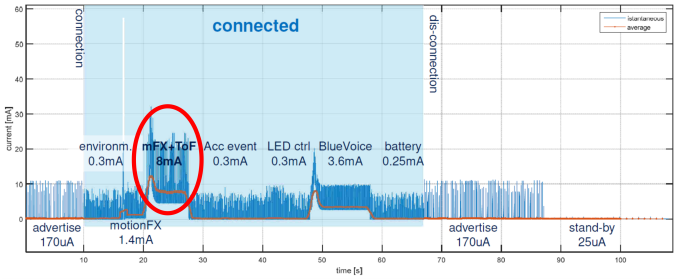

Fig. 9. STEVAL-BCN002V1B average power consumption.

Moreover, it is mandatory to consider the application in which the systems must work. The definition of how and what the system must measure and how often it must send the data to the server is crucial. The working principle of the AIoT node is to store the energy scavenged from the GVEH in the battery. Subsequently, the node uses the battery to power the sensor only when the battery reaches a threshold value of tension. This lower level of the battery charge is imposed by the energetic demand of the user (3 V for the ST unit). The period during which the harvester reaches power level (T) has to be greater than the period during which the power is requested (t) [18]. Consequently, the duty cycle must be defined, consisting in the ratio between the battery discharge time under sensor activity (t) and the recharging time (T). A duty cycle greater than one means that the harvested power is greater than the requested power supply to the sensor, hence the unit can be always active. If the duty cycle is lower than one, the sensor activity schedule must be correctly planned to guarantee the monitoring for the specific application. The battery charge tests results show that, even at high acceleration input and GVEH resonance frequency, the battery is not fully charged at 4.2 V. The blue curve in Figure 8 has an asintote at 3.7 V, still being a valid result for powering the sensor unit. The GVEH can not supply enough current to charge the battery to a voltage above 3.7 V in a significant time period. Hence, the potentially usable capacity of the battery is defined proportionally to the 3.7 V voltage level, obtaining a value of 35.2 mAh respect to the real 40 mAh. Consequently, in real working conditions of the GVEH under different excitations coming from train vibrations, the expected battery charge level and capacity is further lower. The definition of the AIoT node duty cycle needs the comparison between the experimental charge curves at different excitation levels (see Figure 8) and the discharge curve with a current depending on the sensor unit request. The worst scenario of power consumption is considered, where the sensor unit draws the maximum current of 8 mA (see Figure 9 circled in red). The maximum time period of sensor continuos activity (t) results from the discharge curve at maximum current (8 mA) and the minimum voltage threshold to power the sensor (3 V). Table III reports the discharge time up to the threshold, the battery voltage level and the corresponding usable capacity charged in 1.5 hours under the train FFT excitation frequencies and amplitudes, and the duty cycle. The discharge time periods are obtained assuming the discharge curves as linear, both simplyfing the duty cycle definition and considering the worst scenario of a faster discharge process than the real battery behavior. For 0.5 g - 4.2 Hz and 0.16 - 4.0 Hz excitations, the discharge time is equal or greater than the charging one. Hence, the sensor power supply is always guaranteed and no duty cycle needs to be defined, being the battery always over the threshold level. For 0.34 g - 5.8 Hz excitation, the discharge time tends to zero, since the battery level can be charged only up to 3 V threshold value. Consequently, the sensor can never be powered. For 0.16 g - 4.7 Hz, the discharge time is about a third than the charge period. A duty cycle for the sensor activites must be defined to guarantee adequate performance of the whole node. The duty cycle of 0.33 means that in a defined time period the sensor should be on for 33% of the time to allow the battery to be always over the threshold level. The time frame depends on the monitored variable and activity. For istance, in a time frame of one hour, the sensor can be turned on and perform the reading for twenty minutes.

TABLE III
DUTY CYCLE EVALUATION FOR DIFFERENT EXCITATION INPUTS.

Excitation	Battery charge (V)	Capacity (mAh)	Discharge time (h)	Duty Cycle
0.16 g@4.0 Hz	3.1	29.5	0.5	0.33
0.16 g@4.7 Hz	3.3	31.5	1.5	1.0
0.34 g@5.8 Hz	3.0	28.7	0	0
0.50 g@4.2 Hz	3.7	35.2	2.8	1.87

V. Conclusion

An autonomous IoT system prototype for freight trains remote monitoring is described. The generator is a gravitational eletcromagnetic energy harvester (GVEH), able to scavenge vibrations kinetic energy and convert it into electric power. To guarantee a continous monitoring activity under the highly variable train working conditions, a power storage device is necessary. The harvested electric power is rectified, stabilized and stored inside a rechargeable Li-Ion 3.6 V button battery. Laboratory experimental battery charge tests are performed imposing different excitation signals following the experimental freight train FFT. GVEH performance and battery voltage levels are strongly dependent on the excitation input. Battery power is used to supply an ultra-low-power sensor unit (STEVAL-BCN002V1B) for remote monitoring and communication between nodes. Maximum power consumption of the user, and consequent battery discharge time up to the minimum required voltage to power the unit, is compared to the charge time under the main frequencies and amplitudes of the train FFT. The node duty cycle is defined as the ratio between sensor activity time and battery charging time. The results show the potentiality of the GVEH of supplying the user, when excited with the train vibrations, and respecting the duty cycle. The power management system components should be studied more carefully to enhance the energy conversion performances. A refined rectification circuit having lower voltage drop together with a dedicated energy harvesting chip could lead to better results. Future works will regard full scale experimental tests on railway tracks of sensor power consumption during specific monitoring activities. At last, the realization of the WSN with different nodes is necessary to test communication activities and precisely define the power draw and duty cycle of each node.

References

[1] M. Shirvanimoghaddam, K. Shirvanimoghaddam, M. M. Abolhasani, M. Farhangi, V. Z. Barsari, H. Liu, M. Dohler, and M. Naebe. Towards a green and self-powered internet of things using piezoelectric energy harvesting. *IEEE Access*, 7, 12 2017.

[2] A. Dewan, S. U. Ay, M. N. Karim, and H. Beyenal. Alternative power sources for remote sensors: A review. *Journal of Power Sources*, 245:129–143, 2014.

[3] J. Singh, R. Kaur, and D. Singh. Energy harvesting in wireless sensor networks: A taxonomic survey. *International Journal of Energy Research*, 45:118–140, 1 2021.

[4] N. Bosso, M. Magelli, and N. Zampieri. Application of low-power energy harvesting solutions in the railway field: a review. *Vehicle System Dynamics*, 59:841–871, 2021.

[5] Esteban Bernal, Maksym Spiryagin, and Colin Cole. Onboard condition monitoring sensors, systems and techniques for freight railway vehicles: A review. *IEEE Sensors Journal*, 19(1):4–24, 2019.

[6] United States Bureau of Transportation Statistics. Transportation statistics annual report 2022. https://rosap.ntl.bts.gov/view/dot/65841, 2022. Accessed: 2023-02-24.

[7] Z. Hadas, O. Rubes, F. Ksica, and J. Chalupa. Kinetic electromagnetic energy harvester for railway applications - development and test with wireless sensor. *Sensors*, 22(3), 2022.

[8] M. T. Lazarescu and P. Poolad. Asynchronous resilient wireless sensor network for train integrity monitoring. *IEEE Internet of Things Journal*, 8(5):3939–3954, 2021.

[9] S. P. Beeby, R. N. Torah, M. J. Tudor, P. Glynne-Jones, T. O'Donnell, C. R. Saha, and S. Roy. A micro electromagnetic generator for vibration energy harvesting. *Journal of Micromechanics and Microengineering*, 17:1257–1265, 7 2007.

[10] A. Muscat, S. Bhattacharya, and Y. Zhu. Electromagnetic vibrational energy harvesters: A review. *Sensors*, 22, 8 2022.

[11] P. Carneiro, M. P. Soares dos Santos, A. Rodrigues, J. A.F. Ferreira, J. A.O. Simões, A. Torres Marques, and A. L. Kholkin. Electromagnetic energy harvesting using magnetic levitation architectures: A review. *Applied Energy*, 260, 2 2020.

[12] Z. J. Chew, T. Ruan, and M. Zhu. Power management circuit for wireless sensor nodes powered by energy harvesting: On the synergy of harvester and load. *IEEE Transactions on Power Electronics*, 34(9):8671–8681, 2019.

[13] N. Mendiratta, G. Singh, N. Chattoraj, and S. Kundu. Optimization of capacitor for piezoelectric energy harvesting. In *2018 IEEE International Conference on Power Electronics, Drives and Energy Systems (PEDES)*, pages 1–6, 2018.

[14] M. Lo Monaco, C. Russo, and A. Somà. Identification procedure for design optimization of gravitational electromagnetic energy harvesters. *Applied Sciences*, 13(4), 2023.

[15] L. Liu and F. G. Yuan. Diamagnetic levitation for nonlinear vibration energy harvesting: Theoretical modeling and analysis. *Journal of Sound and Vibration*, 332:455–464, 1 2013.

[16] S. Jeba Priya and Daniel Inman. *Energy Harvesting Technologies*. Springer, 01 2009.

[17] M. Lo Monaco, C. Russo, and A. Somà. Numerical and experimental performance study of two-degrees-of-freedom electromagnetic energy harvesters. *Energy Conversion and Management: X*, 18:100348, 2023.

[18] C. Russo, M. Lo Monaco, and A. Somà. Energy harvester duty cycle evaluation for railway vehicle health monitoring. *IOP Conference Series: Materials Science and Engineering*, 1214:012046, 1 2022.